Electronic Supplementary Information (ESI)

Controllable negative thermal expansion, ferroelectric and semiconducting properties in $PbTiO_3$-$Bi(Co_{2/3}Nb_{1/3})O_3$ solid solutions

Hui Liu,[1] Jun Chen,[1] Xingxing Jiang,[2] Zhao Pan,[1] Linxing Zhang,[1] Yangchun Rong,[1] Zheshuai Lin,[2] and Xianran Xing[1]*

[1]*Department of Physical Chemistry, University of Science and Technology Beijing, Beijing 100083, China*

[2]*Beijing Center for Crystal R&D, Key Lab of Functional Crystals and Laser Technology, Technical Institute of Physics and Chemistry, Chinese Academy of Sciences, Beijing 100190, China*

**Corresponding author.Tel.: +86 10 82375027;Email: junchen@ustb.edu.cn.*

Experimental and computational

Materials and synthesis: PT-100*x*BCN (*x* = 0.10-0.42) solid solutions were synthesized by solid-state reaction methods. Analytic reagent grade oxide powders of PbO, Bi_2O_3, Co_2O_3, Nb_2O_5 and TiO_2 (anatase) were selected as starting materials. The well mixed powders were calcined at 850 °C for 5 h. Part of calcined powders were pressed into pellets at a pressure of 200 MPa and sintered at 1060~1100 °C for 2 h covered with the remaining powders to compensate the evaporation loss of PbO and Bi_2O_3 in a covered crucible. After removing the surface layers of the sintered pellets carefully, some of the pellets were ground into powders. Afterwards, the powders annealed at 600 °C for 1 h to remove the mechanical strain introduced during the sintering and grinding procedures.

Characterization: The phase identification was conducted by X-ray diffraction (XRD) with Cu Kα radiation (X'pert PRO, PANalytical). The XRD data for Rietveld refinement were collected with 2θ range 20-120°, step 0.013°, and 20 s/step. The Rietveld refinement of the obtained data was performed on the Fullprof software. High temperature XRD patterns were collected with 2θ range 20-80°, step 0.013°, 20 s/step, which were indexed using Fullprof and DICVOL06 software. UV-vis spectra of surface reflection were measured for powders by Double beam UV-vis spectrophotometer (TU1901, China). The surface morphology of the ceramics was observed by a scanning electron microscope (SEM, LEO1530, Germany). For electrical measurements, electrodes were made by pasting silver on the surface of ceramic disks with 8 mm in diameter and 1 mm in height. Electrochemical impedance spectroscopy (EIS)

measurement was performed at 1 Hz to 1 MHz frequency using a potential of 100 mV with the CHI660E instrument. The ceramics disks were poled under a direct electric field of 6~7 kV/mm for 15 min at 60 °C. After aging 24 h, a quasi-static d_{33} meter (China Academy of Acoustics, ZJ-3) was used to measure piezoelectric coefficient d_{33}. Ferroelectric loops were tested by a ferroelectric tester (model aixACCT, TF Analyzer 1000) at room temperature.

Computational: The first-principles calculations were performed using CASTEP,[1] a plane-wave pseudopotential total energy package based on density functional theory (DFT).[2] Optimized norm-conserving pseudopotentials[3] in Kleinman-Bylander[4] form were employed to model the effective interaction between the atom cores and valence electrons, which allow us to use a relatively small plane-wave basis set without compromising the accuracy required by this study. The Perdew-Burke-Ernzerhof generalized gradient approximation (GGA)[5] functional was adopted to describe the exchange and correlation energy. A high kinetic energy cut off of 800 eV and dense Monkhorst-Pack[6] k-point meshes spanning less than 0.04 $Å^{-1}$ in the Brillouin zones were chosen. Tests show that these computational parameters give results that are sufficiently accurate for purpose of the study. To account for the effect of localized *d* orbitals in Ti, Co and Nb, the GGA+U[7] method with the on-site orbital dependent Hubbard U were employed for the electronic structure calculations. The chosen values of U_d for Ti, Co and Nb are 2.5 eV, 8.0 eV and 6.0 eV, respectively. Virtual crystal approximation (VCA)[8] was adopted to model the cation disordering in PT-40BCN, which has been successfully to study the properties of disordered systems[9-10]

Supplementary Figure S1

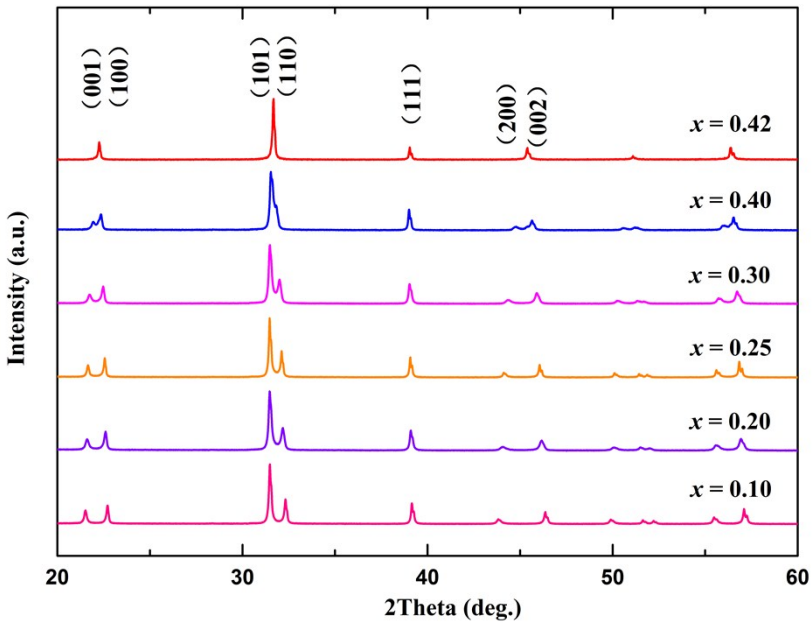

Figure S1. XRD patterns of PT-100*x*BCN (x = 0.10, 0.20, 0.25, 0.30, 0.40 and 0.42) powder.

Supplementary Figure S2

The crystal structures of samples were refined based the Rietveld method by using powder X-ray diffraction. The initial structural model corresponds to $PbTiO_3$ (*P*4*mm*, No. 99) with Pb/Bi at the origin site (0, 0, 0), Co/Ti/Nb are at site (1/2, 1/2, Z_B), and the positions of O(I) and O(II) are at (1/2, 1/2, Z_{O1}) and (1/2, 0, Z_{O2}), respectively.[11,12] The occupancies of atoms were fixed at the nominal composition. The isotropic thermal factors of Pb and Bi, Co, Ti and Nb and O(I) and O(II) were set as equal. The anisotropic profile broadening model suggested by Stephens was taken into account. Beside, in order to take diffuse scattering from ferroelectric domain walls into account, we carried out two-phase model to refine crystal structure.[12-13]

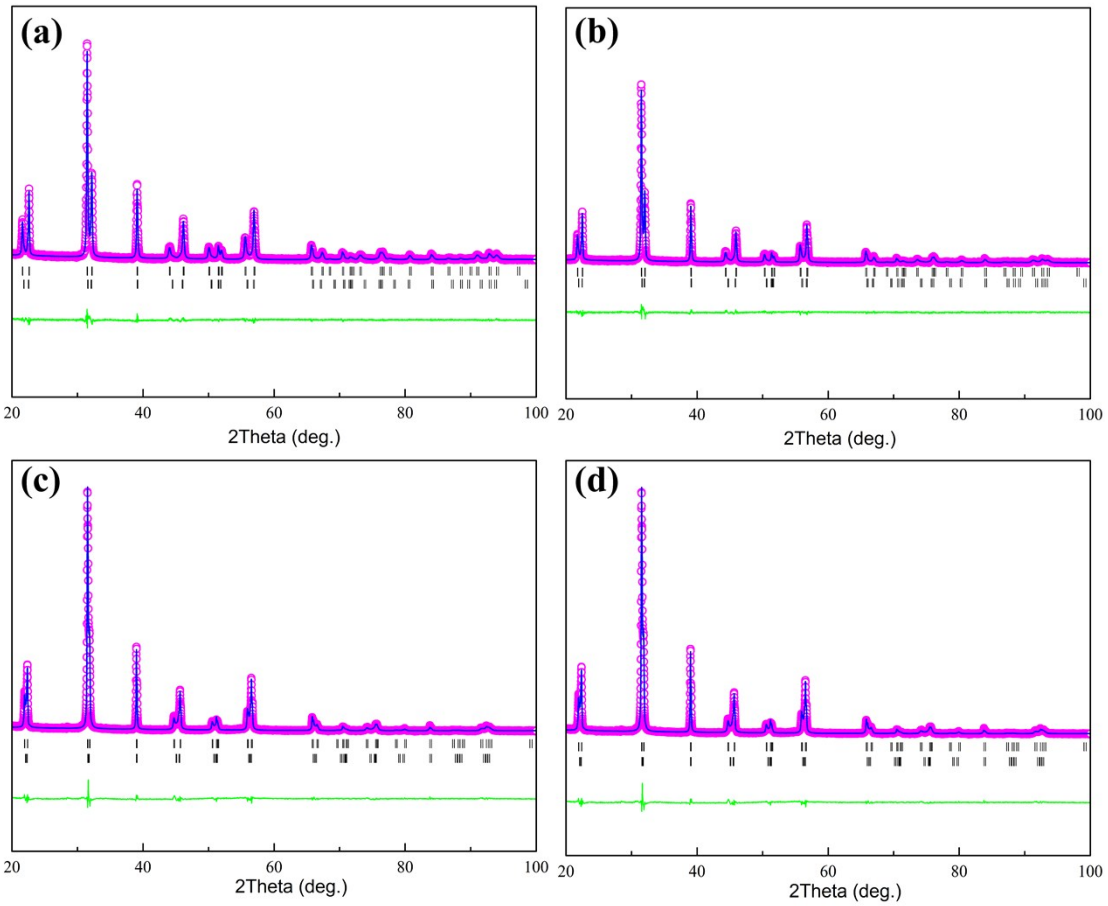

Figure S2. Experimental (circles), calculated (line), and difference (bottom of figure) XRD patterns of the PT-100*x*BCN (x = 0.1, 0.2, 0.3 and 0.4) sample, **(a)** x = 0.1, **(b)** x = 0. 2, **(c)** x = 0.3 and **(d)** x = 0.4.

Table S1. Refined structural parameters of PT-100*x*BCN solid solutions.

Composition		$x = 0.1$	$x = 0.2$	$x = 0.3$	$x = 0.4$
Pb/Bi	Z	0	0	0	0
	B_{iso}	2.8	2.7	3.9	5.0
Co/Ti/Nb	Z	0.54108(79)	0.54418(57)	0.54138(67)	0.54622(59)
	B_{iso}	1.0	1.3	1.3	1.7
O(I)	Z	0.12642(104)	0.11192(102)	0.092683(124)	0.08957(161)
	B_{iso}	1.5	1.7	3.0	4.0
O(II)	Z	0.63053(74)	0.61942(73)	0.60223(98)	0.60048(109)
	B_{iso}	1.5	1.7	3.0	4.0
$a(b)$ (Å)		3.91641(4)	3.93511(5)	3.95314(6)	3.97707(5)
c (Å)		4.12541(5)	4.09605(7)	4.07071(8)	4.03733(7)
c/a		1.053	1.041	1.030	1.015
V (Å^3)		63.28	63.42	63.61	63.86
R_p (%)		14.7	15.5	16.2	16.2
R_{wp} (%)		13.4	12.6	12.9	11.2
χ^2		2.59	1.92	1.77	1.53

Supplementary Figure S3

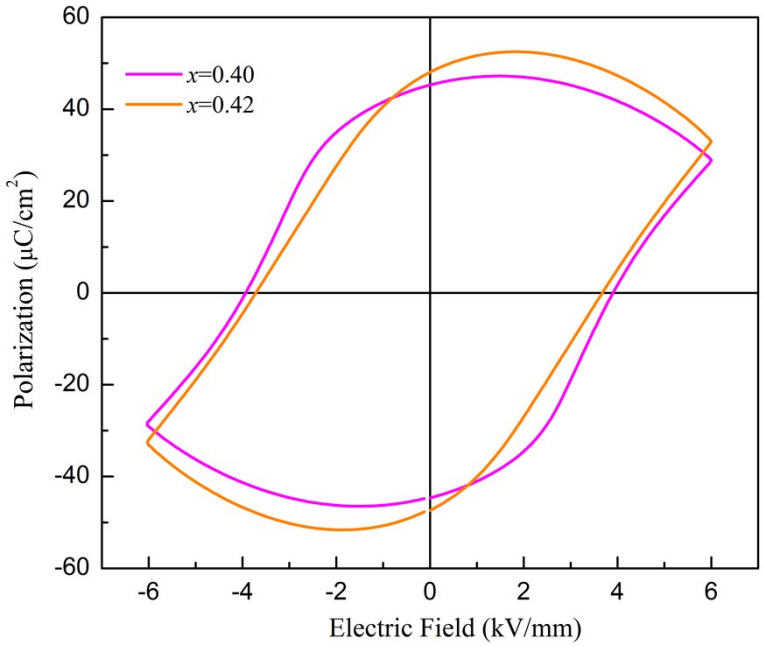

Figure S3. Hysteresis loops of PT-100*x*BCN (x = 0.40 and 0.42) ceramics measured at a frequency of 5 Hz.

Supplementary Figure S4

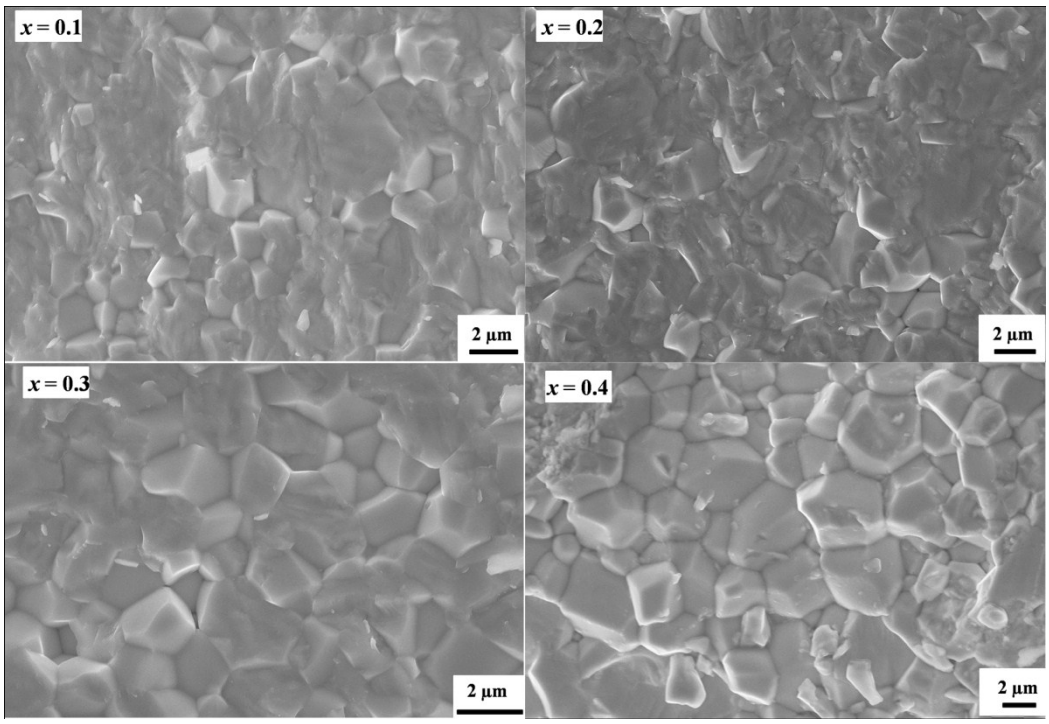

Figure S4. SEM images of PT-100*x*BCN (x = 0.1, 0.2, 0.3 and 0.4) ceramics.

Supplementary Table S2

Table S2. Resistivity at 25 °C, thermistors constant and activation energy of PT-100*x*BCN ceramics

Compositions *x*	R_{25} MΩ·cm	*B* K	E_a eV
x = 0.1	894.0	6318	0.543
x = 0.2	135.8	6189	0.532
x = 0.3	73.2	6508	0.560
x = 0.4	14.7	6311	0.543

Reference

1 S. J. Clark, M. D. Segall, C. J. Pickard, P. J. Hasnip, M. J. Probert, K. Refson and M. C. Payne, First Principles Methods Using Castep. ZKri, 2005, **220**, 567.

2 M. C. Payne, M. P. Teter, D. C. Allan, T. A. Arias and J. D. Joannopoulos, *Rev. Mod. Phys.*, 1992, **64**, 1045.

3 A. M. Rappe, K. M. Rabe, E. Kaxiras and J. D. Joannopoulos, *Phys. Rev. B*, 1990, **41**, 1227.

4 L. Kleinman and D. M. Bylander, *Phys. Rev. Lett.* 1982, **48**, 1425.

5 J. P. Perdew, K. Burke and M. Ernzerhof, *Phys. Rev. Lett.* 1996, **77**, 3865.

6 H. J. Monkhorst and J. D. Pack, *Phys. Rev. B*, 1976, **13**, 5188.

7 V. I. Anisimov, J. Zaanen and O. K. Andersen, *Phys. Rev. B*, 1991, **44**, 943.

8 L. Bellaiche and D. Vanderbilt, *Phys. Rev. B*, 2000, **61**, 7877.

9 N. J. Ramer and A. M. Rappe, *Phys. Rev. B*, 2000, **62**, R743.

10 Y. Deng, R. Z. Wang, L. C. Xu, H. Fang, X. Yang, H. Yan and P. K. Chu, *Appl. Phys. A*, 2011, **104**, 1085.

11 J. Chen, X. Y. Sun, J. X. Deng, Y. Zu, Y. T. Liu, J. H. Li and X. R. Xing, *J. Appl. Phys.* 2009, **105**, 044105.

12 J. Chen, L. Fan, Y. Ren, Z. Pan, J. Deng, R. Yu and X. Xing, *Phys. Rev. Lett.* 2013, **110**, 731.

13 S. Aoyagi, Y. Kuroiwa, A. Sawada, I. Yamashita and T. Atake, *J. Phys. Soc. Jpn.* 2002, **71**, 1218.